INFECTION AND IMMUNITY, Mar. 2008, p. 1036–1047 Vol. 76, No. 3
0019-9567/08/$08.00+0 doi:10.1128/IAI.00985-07

Detection of *Bacillus anthracis* Spore Germination In Vivo by Bioluminescence Imaging▽†

Patrick Sanz, Louise D. Teel, Farhang Alem, Humberto M. Carvalho,‡ Stephen C. Darnell, and Alison D. O'Brien*

Department of Microbiology and Immunology, Uniformed Services University of the Health Sciences, Bethesda, Maryland 20814-4799

Received 18 July 2007/Returned for modification 21 August 2007/Accepted 20 December 2007

We sought to visualize the site of *Bacillus anthracis* spore germination in vivo. For that purpose, we constructed a reporter plasmid with the *lux* operon under control of the spore small acid-soluble protein B (*sspB*) promoter. In *B. subtilis*, *sspB*-driven synthesis of luciferase during sporulation results in incorporation of the enzyme in spores. We observed that *B. anthracis* Sterne transformed with our *sspBp*::*lux* plasmid was only luminescent during germination. In contrast, Sterne transformed with a similarly constructed plasmid with *lux* expression under control of the protective antigen promoter displayed luminescence only during vegetative growth. We then infected A/J mice intranasally with spores that harbored the germination reporter. Mice were monitored for up to 14 days with the Xenogen In Vivo Imaging System. While luminescence only became evident in live animals at 18 h, dissection after sacrificing infected mice at earlier time points revealed luminescence in lung tissue at 30 min after intranasal infection. Microscopic histochemical and immunofluorescence studies on luminescent lung sections and imprints revealed that macrophages were the first cells in contact with the *B. anthracis* spores. By 6 h after infection, polymorphonuclear leukocytes with intracellular spores were evident in the alveolar spaces. After 24 h, few free spores were observed in the alveolar spaces; most of the spores detected by immunofluorescence were in the cytoplasm of interstitial macrophages. In contrast, mediastinal lymph nodes remained nonluminescent throughout the infection. We conclude that in this animal system, the primary site of *B. anthracis* spore germination is the lungs.

The dissemination of infective *Bacillus anthracis* spores in the U.S. mail in 2001 led to 11 occurrences of cutaneous anthrax and 11 cases of inhalational anthrax, with five deaths in the latter group (summarized in reference 20). The impact of this bioterrorism event on those individuals specifically and on society in general provided the impetus for researchers to further define the early steps in establishment of pulmonary anthrax, with the goal of developing potential intervention strategies. One of the first and still considered seminal reports on this subject was published in 1957 by Ross (30). She described the uptake of spores by alveolar macrophages following intratracheal or aerosol delivery in guinea pigs. In that model, infected macrophages were transported to the regional lymph nodes, and germination of the spores within macrophages at those sites was followed by outgrowth and then dissemination of extracellular bacilli.

Even with this fundamental work by Ross, two central issues related to the pathogenesis of anthrax in animal models are sources of controversy. The first point is whether phagocytic cells are required for germination and outgrowth of *B. anthracis* spores. The second question is where does germination occur in pulmonary anthrax? Is it in the lymph nodes or the lungs? To address the first issue, Cote et al. (7) challenged macrophage-depleted mice parenterally with *B. anthracis* spores and observed that those animals died more rapidly than intact mice. These investigators also found that macrophages play a more important role than neutrophils in early host defense against anthrax (7, 8).

Although several studies support the concept that *Bacillus anthracis* spores can germinate within the macrophages (9, 15–17, 39), the fate of the germinated spore and the phagocyte itself are areas in which disparate results have been reported. Some investigators note that germination is followed by replication of bacilli in the macrophage and killing of the phagocytes (9, 31, 39), whereas others observe no replication of the germinated spores in macrophages (16). Still others report that macrophages kill vegetative cells (but not spores) of *B. anthracis* and remain viable (22).

The contribution of other phagocytic cells in the pathogenesis of anthrax has also been proposed. In support of this idea, neutrophils have been shown to phagocytose spores and to permit germination within vacuoles, probably phagosomes (27). Others hypothesize that dendritic cells facilitate the migration of *Bacillus* spores to the mediastinal lymph nodes (4, 5). Indeed, Cleret et al. (6) recently showed that lung dendritic cells can transport spores to thoracic lymph nodes within 30 minutes after intranasal challenge.

There are conflicting reports in the literature about whether spore germination and outgrowth occur in the lungs of intranasally, intratracheally, or inhalationally infected mice (7, 10, 17, 24, 25). To attempt to resolve the discrepant data concerning the site at which germination occurs and the type of innate

* Corresponding author. Mailing address: 4301 Jones Bridge Road, Bethesda, MD 20814. Phone: (301) 295-3400. Fax: (301) 295-3773. E-mail: aobrien@usuhs.mil.

† Supplemental material for this article may be found at http://iai.asm.org/.

‡ Present address: NIH/NIAID, 6700-B Rockledge Dr., Room 4218, Bethesda, MD 20892.

▽ Published ahead of print on 14 January 2008.

immune cell(s) associated with spore germination, we sought to develop a *Bacillus anthracis* infection model in which to visualize the potential location of and cellular response to germination in a living animal. Bioluminescent *Bacillus subtilis* in which the *luxAB* operon from *Vibrio harveyi* is expressed under the control of the *sspB* spore promoter was previously described (32). In that system, light emission is observed to correspond with germination in vitro; however, the luminescence reporter requires addition of exogenous luciferase substrate for light detection. More recently, the *lux* operon from *Photorhabdus luminescens* was cloned into various gram-negative and gram-positive bacteria (*Pseudomonas aeruginosa* [21], *Escherichia coli* O157:H7 [34], *Staphylococcus aureus* [12, 21], *Streptococcus pneumoniae* [13], or group A streptococcus strain 591 [28]). In these cases, the entire *lux* operon that encodes luciferase and its substrate is incorporated such that exogenous substrate is not necessary, a modification that makes this operon more suitable for in vivo studies. We describe here the construction of bioluminescent *Bacillus anthracis* Sterne strains in which the *lux* operon was temporally expressed such that light was detectable on germination (germination reporter strain) or, as a control, during vegetative growth (vegetative reporter strain). The germination reporter strain was used to identify discrete and localized sites of germination within the lungs of infected mice during the course of infection by in vivo imaging. Luminescence from this strain was detected in situ, and the affected tissues were evaluated by cytological, histological, and bacteriological staining. Our observations, in contrast to a very recent report by Glomski et al., who used a vegetative cell reporter strain (14), indicate that germination occurs in lung tissue within 30 min of intranasal challenge. We also show that alveolar macrophages appear to be the first cell type in contact with spores and that polymorphonuclear cells are the predominant phagocytic cells associated with spores late in infection.

MATERIALS AND METHODS

Bacterial strains and DNA manipulations. *B. anthracis* Sterne strain 34F2 ($pXO1^+$ $pXO2^-$; obtained from Robert Bull, Naval Medical Research Center) was used for in vitro and in vivo experiments. Recombinant DNA techniques were conducted in *E. coli* strain DH5α (Invitrogen, Carlsbad, CA). Unmethylated plasmid DNAs were prepared from *E. coli* strain JM110 (Stratagene, La Jolla, CA). PCRs were done with the Expand High-Fidelity PCR system (Roche Diagnostics, Indianapolis, IN) in a PTC200 Peltier thermal cycler (MJ Research, Bio-Rad, Hercules, CA). Genomic DNA was extracted from *B. anthracis* strains using the Easy-DNA kit (Invitrogen, Carlsbad, CA), and plasmid DNA was purified using a QIAEX II gel extraction kit (Qiagen, Valencia, CA). DNA sequences were verified with the ABI Prism Big Dye method (Applied Biosystems, Foster City, CA) by the Biomedical Instrumentation Center at the Uniformed Services University.

Construction of luminescence reporter plasmids. The episomal reporter plasmids used in this study were derived in several steps from precursor plasmids originally designed to integrate the *lux* reporter cassettes into the *B. anthracis* chromosome within the native *Bacillus* β-lactamase gene (locus BAS2328). The plasmids used in or generated during this study are summarized in Table S1 of the supplemental material. The steps in assembly of the plasmid intermediates are also described in the supplemental material. To summarize, components of the bioluminescence reporters were amplified by PCR from the sources that follow and then spliced together by overlap extension with the primers shown in Table S2 of the supplemental material. A promoterless *luxABCDE* cassette flanked on the 3′ end with a kanamycin resistance marker was derived by PCR from pXEN5 provided by Xenogen Inc. (12, 13). The protective antigen (PA) gene promoter was amplified from pYS5, a *Bacillus* vector that encodes *pag*; that recombinant plasmid was graciously provided by S. Leppla (33). The *B. anthracis* Sterne gene homologous to the small acid-soluble protein gene in *Bacillus subtilis* is locus BAS0815 (hereafter also called *sspB*). The promoter region of *sspB* was amplified from genomic *B. anthracis* Sterne DNA. Plasmid pYS5 was digested with ApaI-BamHI to release the PA-encoding sequence, and the 5.4-kb backbone DNA was reserved. A 1-kb PCR product was amplified (from pYS5) with mutagenic primers to introduce an ApaI site and SalI, NotI, and BamHI sites on either end. Following treatment of this fragment with ApaI and BamHI, the DNA segment was ligated into the corresponding ends of the pYS5 vector backbone to create pYS-NSB, an *E. coli*/*B. anthracis* shuttle vector for episomal expression in *B. anthracis*. The addition of NotI and BamHI restriction sites in the formation of pYS-NSB facilitated the incorporation of the *lux* reporter cassettes encoded on 5.8- or 5.9-kb NotI-BamHI fragments from precursor plasmids pPS10 and pPS9, respectively. The resultant reporter plasmid with the PA promoter-driven *lux* cassette was named pPS11 (the vegetative reporter), and the *sspB* promoter-driven reporter plasmid was named pPS12 (germination reporter).

Transformation of *B. anthracis* with luminescence reporter plasmids. Plasmids (pPS11, pPS12, or the shuttle vector pYS-NSB alone) were electroporated into *B. anthracis* with selection for kanamycin resistance as described by Koehler et al. (23), with some modifications as indicated below. Briefly, 0.8 ml of an overnight *B. anthracis* Sterne culture was transferred into 25 ml of brain heart infusion (BHI) broth that contained 0.5% glycerol, and the bacterial culture was then incubated with shaking until the optical density at 600 nm (OD_{600}) reached 0.6. Cells were harvested by filtration, washed three times with 25 ml of ice-cold electroporation buffer (1 mM HEPES, 10% glycerol, pH 7.0), and resuspended in 1.25 ml of electroporation buffer. Five μg of unmethylated plasmid DNA was mixed with 0.3 ml of the cell suspension on ice, and the DNA was electroporated into the bacteria with a Bio-Rad gene pulser (2.5 kV, 25 μF, 800 Ω). The resultant suspension with potential transformants was then incubated in 1 ml of BHI with 10% glycerol, 0.4% glucose, and 10 mM $MgCl_2$ buffer for 2 h with shaking at 37°C and spread onto kanamycin BHI agar plates. Colonies of *Bacillus anthracis* successfully transformed with pPS11 or pPS12 were identified on BHI plates with kanamycin by luminescence when scanned for 1 minute with a charge-coupled device (CCD) within the Xenogen In Vivo Imaging System (IVIS) detection chamber (Xenogen Corporation).

Generation and purification of luminescent *B. anthracis* spores. Single colonies of *B. anthracis* Sterne strain 34F2 or 34F2 transformed with pPS11 or pPS12 were taken from trypticase soy agar (TSA) and inoculated into TS broth (TSB) for culture overnight at 37°C. Each culture was spread onto modified germination (G) medium agar plates [0.2% yeast extract, 0.2% $(NH_4)_2SO_4$, 1.5% Bacto agar, 0.0025% $CaCl_2$ dihydrate, 0.05% K_2HPO_4, 0.02% $MgSO_4$ heptahydrate, 0.005% $MnSO_4$ quatrahydrate, 0.0005% $ZnSO_4$ dihydrate, 0.0005% $CuSO_4$ pentahydrate, 0.00005% $FeSO_4$ heptahydrate] with 50 μg/ml kanamycin. The plates were incubated at 30°C for 8 to 10 days in the dark. Colonies scraped from the surface of the agar were resuspended in distilled water and were heat treated at 65°C for 1 h to kill any viable vegetative cells. Purification of spores was done with 58% (vol/vol) Renografin (Renocal-76 diluted in distilled H_2O; Bracco Diagnostics, Princeton, NJ). Spores were layered onto the 58% Renografin and centrifuged at 6,000 × *g* for 30 min in a swinging bucket rotor. The sedimented spores were washed twice with distilled water. After the final sedimentation, the spores were resuspended in distilled water to yield a final concentration of 10^9 to 10^{10} spores/ml, as determined by vegetative outgrowth on TSA plates.

Characterization of the *Bacillus anthracis lux* operon reporter strains. The temporal expression of luminescence from the *B. anthracis* spores transformed with either pPS11 or pPS12 was monitored by quantitation of photon emissions by the IVIS CCD camera over time. Spore solutions were incubated with germination solution (0.25 mM L-alanine, 1 mM inosine) or BHI broth in a total volume of 200 μl in a 96-well plate at 37°C. Luminescence was recorded with 1-min exposure times every 5 to 10 min for 13 h. The emission of photons from selected and defined areas of triplicate samples was quantified using the Living Image 2.5 software package (Xenogen Corporation) and graphed using Microsoft Office 2000 Excel.

Vegetative growth patterns of the parent *B. anthracis* Sterne strain and the parent strain transformed with pPS11 were determined by measurement of the OD_{600} of TSB cultures at various times over 8 hours. Germination efficiencies of the *sspBp*::*lux* reporter strain, vector-alone strain, and the host Sterne strain were compared by culturing spores in 5% BHI broth, taking samples from the broth cultures at various time points, and heat inactivating the vegetative cells at 68°C for 1 h, as described by Brahmbhatt et al. (3). The heat-treated broth was then subcultured onto BHI agar to enumerate the residual heat-resistant spores. The decline in heat-resistant CFU over time was tested for both strains in three independent experiments. Within each experiment, three samples of each strain

were heat treated and counted, and the geometric mean CFU for like samples was determined.

Inoculation and observation of luminescence in infected mice. Six- to 8-week-old female A/J mice, purchased from The Jackson Laboratory (Bar Harbor, ME), were used throughout the study. To immobilize mice for observations in the IVIS instrument, isoflurane anesthesia was administered to mice with the XGI-8 gas anesthesia system (Xenogen Corporation). For subcutaneous inoculations, 100 μl of spore suspension of about 10^9 CFU/ml was delivered via tuberculin syringes fitted with a 29-gauge needle into the loose skin on the backs of mice as previously described (41). For intranasal spore challenge, mice were sedated with isoflurane as described above or with 2 mg ketamine and 0.3 mg xylazine administered intraperitoneally in a 100-μl aqueous solution. Twenty-five to 50 μl of spore suspension of varied concentrations (see below) was placed on the nares of anesthetized mice, and the mice were held upright until the inoculum was inhaled. The 50% lethal doses (LD_{50}s) of luminescent and untransformed *B. anthracis* Sterne spores by both subcutaneous and intranasal routes were determined by treatment of groups of five mice each with doses of spores that ranged from $\sim 10^3$ to 10^5 spores for subcutaneous infection and $\sim 10^5$ to 10^7 for intranasal inoculation. The minimum dose of the reporter strain that resulted in luminescence in live mice was 10^4 spores administered subcutaneously and 10^7 spores administered via the intranasal route. For in vivo live imaging, mice were positioned within the IVIS detection chamber on their backs such that they received continuous isoflurane sedation through the nose cones of a gas anesthesia manifold within the imaging chamber. A luminescence signal was acquired for a maximum of 5 min using an IVIS CCD camera. At selected times postinfection, mice were euthanized by cervical dislocation while sedated. Under the direction of a veterinarian, the lungs were dissected from the mice with the tracheobronchial lymph node intact at the tracheal bifurcation, as described by Van den Broeck et al. (38). Following removal of the lungs, the caudal mediastinal node was also excised. All the extracted tissues were scanned for luminescence using the IVIS for a maximum time of 5 min. Luminescent and nonluminescent lung tissues from infected mice and uninfected control mice were divided in half with a scalpel. A portion was quick-frozen in liquid nitrogen and then embedded in optimum cutting temperature compound (Sakura, Torrance, CA). Tissue blocks were stored at −80°C and thinly sectioned (6 to 8 μm) to prepare slides for immunohistochemistry. The cut aspect of the remaining tissue portion was blotted onto clean microscope slides to prepare tissue imprints as described elsewhere (36).

Determination of CFU. To assess the concentration of *B. anthracis* in tissue after infection, lung tissues from infected mice were weighed and homogenized in 10 ml of sterile water. A portion of the homogenate was serially diluted and spread on BHI plates to assess the total number of microorganisms (spores and vegetative cells) per gram of tissue. Another fraction of the lung homogenate was diluted in preheated sterile water, held at 68°C for 1 h, and then serially diluted and cultured as above to enumerate the spores.

Microscopic tissue analysis. Frozen sections of mouse lung tissue or tissue imprints of dissected tissue were subjected to immunostaining as follows. Slides were blocked with 3% bovine serum albumin (Sigma, St. Louis, MO) in phosphate-buffered saline (PBS) overnight at 4°C and incubated with the correct primary antibody for 60 min at room temperature. Sections were washed twice with PBS for 5 min, incubated with the appropriate secondary antibody for 60 min at room temperature, washed again with PBS, and then allowed to air dry for 20 min. The samples were then mounted in Fluoromount-G (SouthernBiotech, Birmingham, AL). Immunofluorescence was observed with a Zeiss inverted confocal laser scanning microscope. The antibodies used included anti-BclA (*B. anthracis* exosporium glycoprotein) polyclonal antibody (3), anti-*B. anthracis* vegetative cell protein EA1 (42) (clone SA26; Abcam, Cambridge, MA), anti-macrophage cell marker CD68 (clone FA-11; Serotec, Raleigh, NC), Alexa 488-conjugated goat anti-mouse immunoglobulin G (IgG; Molecular Probes, Carlsbad, CA), Alexa 594-conjugated goat anti-rat IgG (Molecular Probes), and Alexa 488-conjugated goat anti-rabbit IgG (Molecular Probes). To stain eukaryotic nuclear DNA, we used 4′,6-diamidino-2-phenylindode, dihydrochloride (DAPI; Molecular Probes). Tissue imprint slides were subjected to the Wirtz-Conklin spore stain (18), a process in which 5% aqueous malachite green solution is applied with gentle heating for 5 minutes followed by 0.5% aqueous safranin counterstain. Endospores are readily distinguished as green spherules, in contrast to vegetative cells, phagocytic cells, and cellular debris, which retain the red safranin counterstain. Stained lung imprints from mice dissected at 30 min, 1 hour, 6 h, 24 h, and 48 h postinfection were viewed under oil immersion at 100× magnification to enumerate polymorphonuclear leukocytes and macrophages with and without intracellular spores. Two blots were made of each tissue sample, and 50 oil immersion fields on each blot were counted.

Statistical evaluations. The LD_{50} of the strains used in these experiments was calculated according to the method of Reed and Muench (29). The vegetative growth curves of the parent and the germination reporter strains were generated by plotting the average outcome (OD_{600}) of three experiments per strain. To compare differences in germination rates among strains, changes in $\log_{10}$ counts of bacteria from t_0 to t_x were compared using a one-way analysis of variance (ANOVA) followed by Tukey's pairwise post hoc comparisons.

RESULTS

Temporally expressed *lux* reporter plasmids. *B. anthracis* reporter strains designed to exhibit bioluminescence during either germination or vegetative growth were constructed. In each case, the complete *luxABCDE* cassette was introduced into a *Bacillus*/*E. coli* shuttle vector that was then electroporated into the *B. anthracis* Sterne strain; therefore, addition of exogenous substrate to display luciferase activity in the transformants was not necessary. Reporter plasmid pPS11 exploited the vegetative PA promoter upstream of *lux* to signal vegetative growth. In pPS12, the *B. anthracis* homologue of the *sspB* promoter, previously shown to signal early steps in *Bacillus subtilis* germination, was inserted upstream of *lux* for detection of spore germination. Insertion of the reporter cassettes onto the *B. anthracis* Sterne strain chromosome within the β-lactamase gene was also considered. We reasoned that the reporters would be stably incorporated as a single copy in that gene in the absence of antibiotic selection. However, we could not be certain whether other factors might influence expression at that insertion site, nor was it clear that adequate signal would be detectable in vivo with a single-copy reporter cassette; therefore, we conducted the in vivo infection studies with reporters borne episomally in *B. anthracis* Sterne.

Spores were derived from *Bacillus* transformed with pPS11 (vegetative reporter) or pPS12 (germination reporter) under antibiotic selection to assure the retention of the *lux* reporter plasmids during sporulation. These spores were used to establish the kinetics of expression from the *lux* reporters with the IVIS instrument during germination and growth in broth in 96-well microtiter plates. Luminescence during growth in BHI broth, a medium that supports both germination and vegetative outgrowth, was compared with growth in minimal defined germination medium that permits germination but not vegetative growth (Fig. 1). In the BHI assay (Fig. 1A), luminescence peaked between 30 and 90 min for pPS12 and at about 3 hours for pPS11, an indication that *lux* expression in pPS11 and pPS12 was temporally regulated as predicted. As expected, the vegetative promoter-driven *lux* reporter strain emitted light only in BHI. In the germination medium, where only the early stage of germination can occur (1, 40), there was no outgrowth into vegetative cells and therefore no *lux* expression or light emission from the PA vegetative reporter (Fig. 1B). Light emission from the germination reporter was detectable with the IVIS after only 5 minutes of incubation. Such early bioluminescence (in medium that does not support vegetative growth) indicated that the LuxA, -B, -C, -D, and -E proteins encoded on pPS12 were packaged in the spores, remained stable, and were active upon germination, as is the case for the native SspB protein that is expressed during sporulation and packaged in the spore itself. Germination in the presence of protein synthesis inhibitors resulted in a reduced light emission (R. Cybulski, P. Sanz, and A. O'Brien, unpublished data);

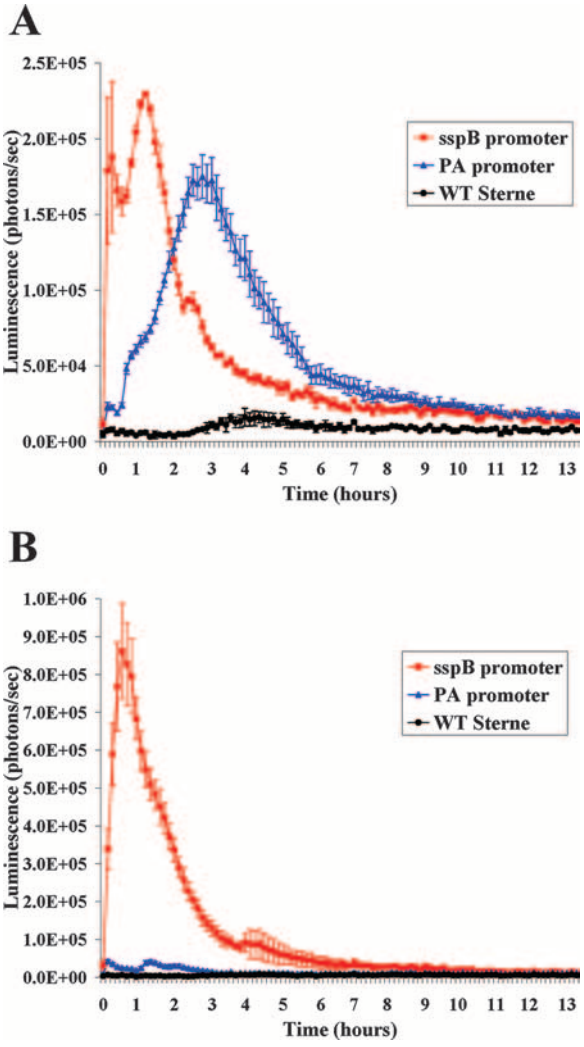

FIG. 1. Luminescence of *Bacillus anthracis* Sterne strain transformed with the germination *lux* reporter plasmid pPS12 (*sspB* promoter) or the vegetative *lux* reporter plasmid pPS11 (PA promoter) measured during overnight culture in BHI (A) or germination medium (B), as detected by the Xenogen IVIS (values are reported as photons/s captured over the area of each well). The curves represent the means of three assays, and the error bars indicate ± 1 standard deviation per time point.

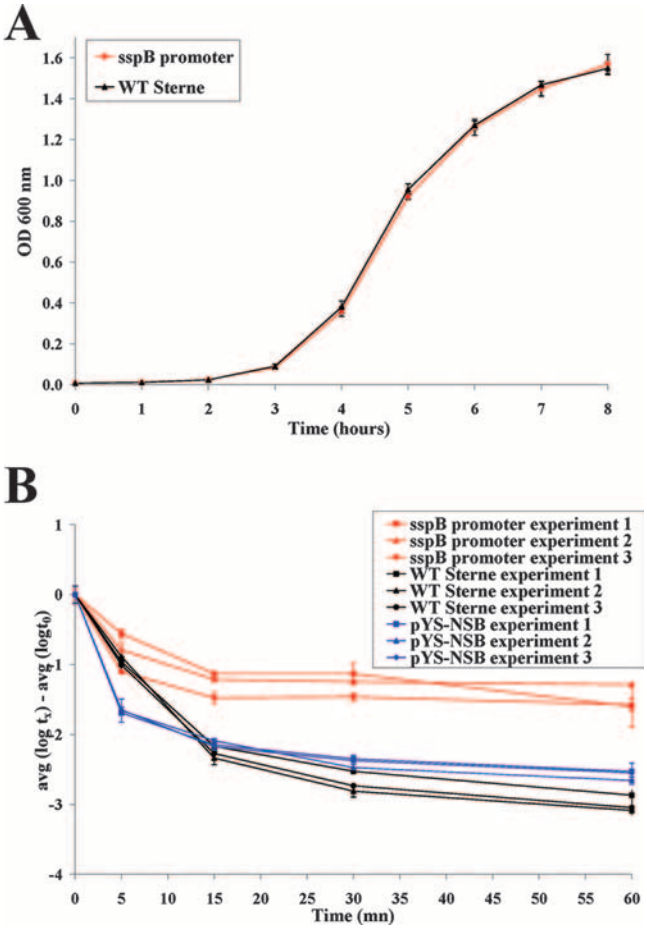

FIG. 2. (A) Comparison of the wild-type Sterne strain and that strain transformed with pPS12 during vegetative growth in TSB over time (mean of three independent experiments shown with error bars to indicate ± 1 standard deviation). (B) Kinetics of germination of spores from the parent strain, the parent strain transformed with pYS-NSB, and the germination reporter strain. Spores were grown in 5% BHI broth, and samples were heat treated to inactivate vegetative cells at the time points shown. Colony counts following heat treatment represent the numbers of heat-resistant spores. The difference between the spore counts at the starting point (t_0) and those at subsequent test points (t_x) indicates the number of spores that germinated at each time point (error bars represent variations among three like samples at each time point ± 1 standard deviation). The germination curves for three individual experiments are shown. The level of *sspBp*::*lux* reporter germination at 60 min (in red) is statistically lower than for the wild type (in black) ($P < 0.001$), as well as for the wild type with vector alone (in blue) ($P < 0.001$). There is also a difference in germination at 60 min between the wild type (black) and the wild type with vector alone (blue) ($P = 0.016$).

therefore, we reasoned that some bioluminescence during germination resulted from new protein synthesis, probably from RNA molecules also trapped in the spore during sporulation. As a negative control, spores were incubated in water, and no luminescence could be detected despite incubation for up to 14 h (data not shown).

Because our primary interest was to study the very early stages of *Bacillus* infection in vivo, we proceeded to focus on the germination reporter strain and compared its in vitro growth properties with those of the parent Sterne strain. We determined that the vegetative growth curves for the two strains were indistinguishable (Fig. 2A). In contrast, we noted in vivo that the LD_{50} for the reporter strain was higher than that of the wild-type Sterne strain (as described below), an observation not predicted by the vegetative growth assessment.

To determine if the reporter strain was as germination competent as the wild-type *B. anthracis* Sterne strain, we compared the germination rates of the parent strain and the strain transformed with either pPS11 or the vector (pYS-NSB) alone in vitro. The proportion of spores from the vector-transformed strain that underwent germination was somewhat reduced compared to the germination levels observed with the parent strain (Fig. 2B). Germination of the Lux reporter strain was significantly reduced compared to its parent strain or the parent transformed with vector alone (Fig. 2, *P* values). Nonethe-

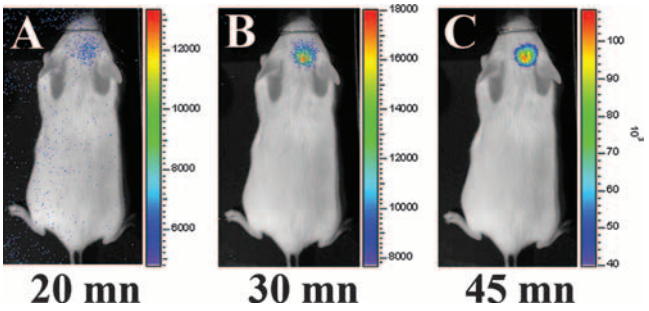

FIG. 3. Bioluminescence detected in mice inoculated subcutaneously (in skin over the head/neck area) with *B. anthracis* Sterne that was transformed with the germination *lux* reporter plasmid pPS12. Mice were monitored with the Xenogen IVIS at 20 min (A), 30 min (B), and 45 min (C) postinoculation. Merged photographic and luminescence images are shown. Note that the signal intensity in panel C is highest and is expressed in units $\times 10^3$. Luminescence is reported as photons per second per square centimeters per steradian.

less, the proportion of spores of each strain that had germinated after 1 hour was 99.90% for the wild type, 99.74% for the vector-alone strain, and 96.75% for the *sspB* promoter-driven *lux* reporter strain. Therefore, we reasoned that despite reduced germination efficiency in the reporter, the bulk of spores were capable of germination and establishment of lethal infection in mice, and so subsequent in vivo studies were undertaken.

In vivo expression of *lux* during *Bacillus* infection of mice. To assure that the *lux* operon was expressed and that luminescence was detectable in a live mouse, we first infected A/J mice by the subcutaneous route as previously described (41). The calculated LD_{50} by the subcutaneous route for the wild-type Sterne strain was 2.3×10^3 CFU, whereas the LD_{50} for the luminescent strain was 1.5×10^4 CFU by that route. Luminescence was detectable in a live animal as early as 20 min after infection near the site of injection (Fig. 3) with an inoculum of 6×10^7 CFU. This result indicated that germination had occurred and that the IVIS effectively captured the luminescent signal from the live infected animal.

Next, to study anthrax germination in the context of a pulmonary infection with the *lux* germination reporter strain, the mice were challenged with spores intranasally. We determined that the recombinant strain transformed with pPS12 had an LD_{50} of 1.4×10^6 CFU and the wild-type Sterne strain LD_{50} was 6.7×10^4 CFU by the intranasal route. The increased LD_{50} of the transformant by both the subcutaneous and intranasal routes was consistent with the reduced germination efficiency of the reporter strain that we observed in vitro. We then challenged mice after anesthesia with $\sim 1 \times 10^7$ CFU of the germination reporter (about 10 LD_{50}s) intranasally and regarded the live animals under sedation starting at 30 min postinfection and at various intervals up to 4 days. Table 1 summarizes the frequency and time of appearance of luminescence in these mouse experiments. A representative 48-hour kinetic study of five mice is shown in Fig. 4A. When luminescence was observed in live mice, it was consistently localized to the ventral pulmonary region (left or right). Although mice displayed luminescence at differing rates and mouse 1 was never observed to be luminescent, all of the mice in this experiment died. We reasoned that mouse 1 was infected but the infective dose was below the detectable luminescence threshold, or that luminescence was expressed during an interval when that animal was not being screened with the IVIS. The earliest evidence of luminescence in live mice was observed at 18 h (Fig. 4B). Luminescence remained detectable in live animals between 2 and 4 days after infection (data not shown). In some cases the light signal disappeared over time and before the death of the animal, but in other cases animals showed luminescence until death. This variation might reflect a difference in the extent of germination in different animals. To control for the potential that inhalation of isoflurane anesthesia might in itself contribute to germination of the reporter spores, a subset of mice were anesthetized with ketamine intraperitoneally prior to spore challenge and their tissues were evaluated for luminescence. No difference was seen in the frequency, location, or time of appearance of luminescence with ketamine anesthesia (Table 1). Bioluminescence was measured during intranasal infection with the vegetative (*pag*::*lux*) reporter strain as well. With that construct, luminescence was detectable as early as 18 to 20 h and was confined to the lungs of infected animals. However, the signal was more intense than the germination signal, a finding consistent with vegetative replication (data not shown).

Localization of the site of germination. Necropsy of infected luminescent mice allowed us to better define the origin of the germination reporter signal. Once the overlying tissues were retracted, the source of light emission was sharper and confined to distinct foci in the lobar lung tissue of the infected A/J mice (Fig. 5). This luminescent lung tissue was distinguishable from the nonluminescent lymph tissue at the tracheal bifurcation (not shown). After removal of the lungs, the caudal mediastinal lymph node was dissected from each mouse, but none of these excised nodes was luminescent when scanned with the IVIS (Fig. 5C and D show a representative sample). The IVIS was also used to further isolate the luminescent portions of the lungs for microscopic studies (Fig. 5C and D). Dissection was performed on mice euthanized at early time points after infection to detect luminescence in situ before mice showed gross

TABLE 1. Summary of *Bacillus anthracis* germination reporter luminescence observed postinfection in live mice or in tissues from infected mice

Expt no.	Anesthetic	Time postinfection (h)	Frequency of luminescence		
			In live animals	In situ[a]	On dissection of tissue
1	Isoflurane	1	Not imaged	Not imaged	2/8
	Isoflurane	2	Not imaged	Not imaged	6/8
	Isoflurane	4	Not imaged	Not imaged	6/8
2	Isoflurane	0.5	Not imaged	Not imaged	3/4
	Isoflurane	1	Not imaged	Not imaged	2/4
	Isoflurane	6	Not imaged	2/4	4/4
	Isoflurane	24	0/4	2/4	3/4
	Isoflurane	48	1/4	1/3	3/3
3	Ketamine	1	Not imaged	Not imaged	1/3
	Ketamine	6	Not imaged	2/5	4/5
	Ketamine	72	1/4	Not imaged	4/4

[a] Euthanized animals were imaged after the abdomen and thorax were opened to reveal respiratory and digestive tracts and prior to extraction of tissues.

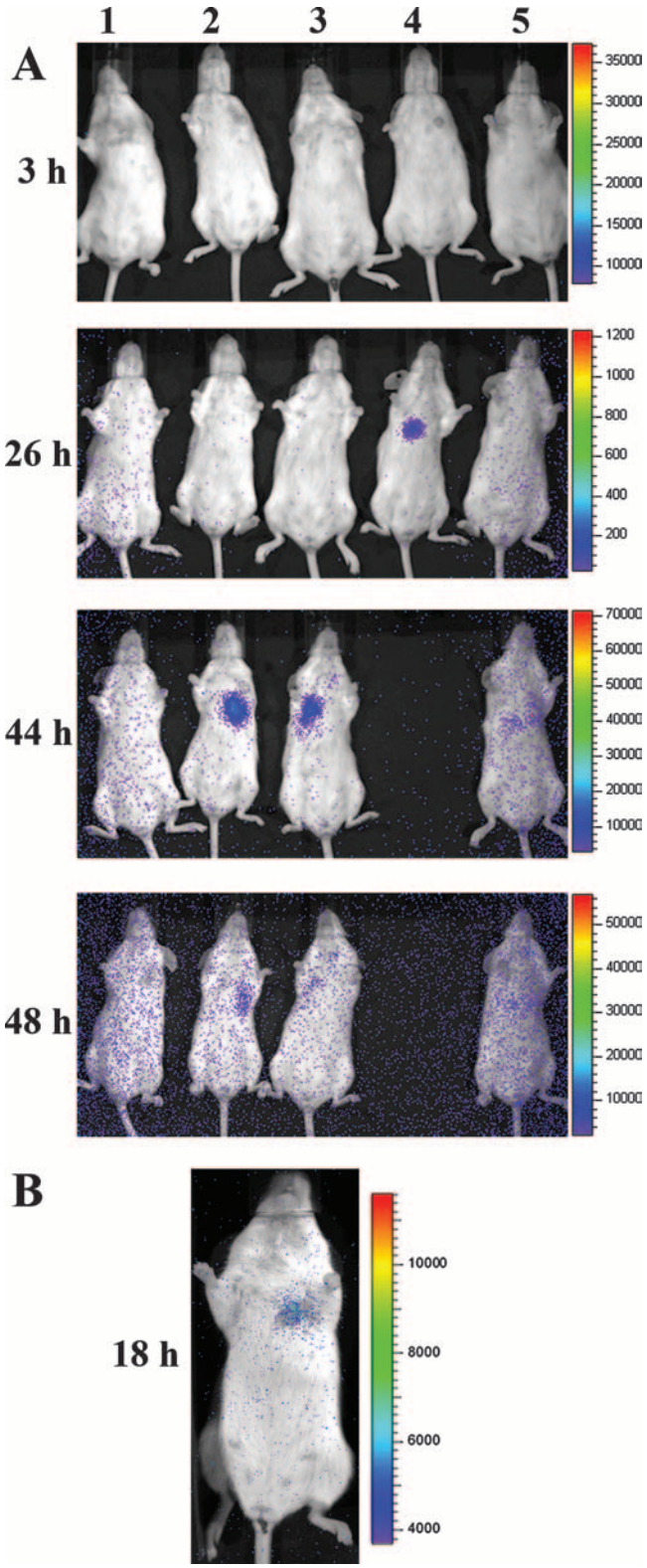

FIG. 4. Merged luminescent and photographic images of mice after intranasal inoculation with ~1 × 10^7 *B. anthracis* spores transformed with pPS12. (A) Evidence of germination in the ventral thorax of three of five mice (animals 2, 3, and 4) within 48 h of infection. Mouse 5 appeared to have increased luminescence over the same area at 44 h, but the signal was weaker than with mice 2, 3, and 4. Mouse 4 died prior to the 48-h postinfection measurement. Note that for mice 2 and 3 the signal was on at 44 h and then off or decreased at 48 h, a pattern that is expected for a system that monitors spore germination but not vegetative cell outgrowth. Visualization of the low level of luminescence at 48 h was enhanced by increasing the background sensitivity, an adjustment that resulted in a generalized increase in background signal (blue dots) that is artificially concentrated around the periphery. (B) In a separate experiment, bioluminescence was detectable in one mouse at 18 h postinfection.

luminescence. As early as 6 hours postinfection, foci of light emission were seen in the lungs of some sacrificed mice before the tissue was disturbed or removed from the thoracic cavity (data not shown). In others, the lung tissue was excised and then scanned with the IVIS. The earliest observation of luminescence from a germination reporter strain in extracted lung tissue was at 30 min postinfection. The microscopic findings from those tissues are discussed in the following section.

Microscopic examination of luminescent tissues. In all the infected mice analyzed, the lungs were the only organs in which luminescence could be detected. Luminescent and nonluminescent tissues were removed from infected mice after sacrifice. Lung tissues from uninfected control mice were also examined. Slide tissue imprints of lung sections were subjected to Wirtz-Conklin spore stain and immunofluorescence staining with antibodies specific for CD68 on macrophages, BclA, the hair-like nap on the exosporium of spores (37), and EA1, a predominant vegetative cell antigen (11). Flash-frozen tissue sections were also stained for immunofluorescent detection of macrophages, spores, and vegetative cells as above. Tissue blotted on slides permitted better recovery and visualization of host cell types and bacterial morphologies, while frozen tissue sections allowed us to localize the cellular and bacterial antigens within the tissue architecture.

The phagocyte populations differed in tissues sampled at various times postinfection (Table 2). In lung imprints made at 30 min and 1 hour postexposure, macrophages with apparently intracellular malachite green-stained spores were seen along with numerous extracellular spores (Fig. 6A and B, 1 h). At 6 hours postexposure, there was a dramatic increase in polymorphonuclear leukocytes (PMNs), and many contained intracellular spores (not shown). The observation of enhanced recruitment of PMNs was sustained through 48 h (Fig. 6C and D, 24 h). Vegetative cells were also seen on spore stains of lung tissue imprints, but they did not appear to be intracellular (not shown).

In frozen sections of lung tissue collected at 30 min after infection, spores were seen extracellularly and associated with macrophages in alveolar spaces. There was no microscopic evidence of structures resembling lymphoid tissue (Fig. 7A, B, and C). This observation was consistent with the results of spore stains from tissue imprints at the same time point. Vegetative cell antigen also was seen colocalized with macrophages at this early time point (Fig. 7D, E, and F). Tissue imprints from infected lung harvested at 48 h and subjected to fluorescent antibody staining showed that neutrophils were present along with macrophages and that the PMNs also contained spores (Fig. 8A, B, and C). This latter finding was consistent with spore stains of tissue imprints at 48 h (Fig. 6C and D). In frozen tissue sections taken at 48 h, macrophage and PMN

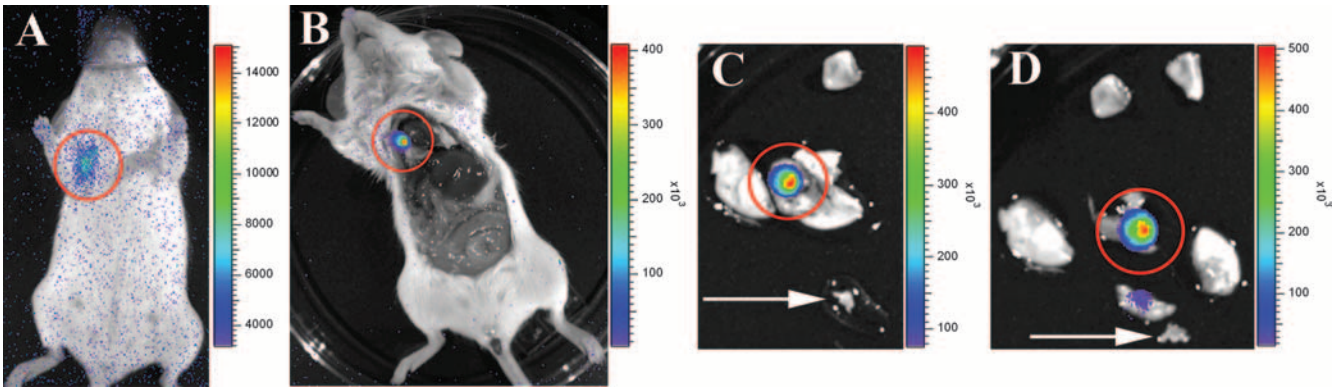

FIG. 5. Bioluminescence observed 48 h post-intranasal inoculation with spores of *B. anthracis* transformed with pPS12 in a live mouse (A), after euthanasia and exposure of the chest cavity (B), and in whole lung tissue and in dissected lung segments (C and D, respectively), where the *lux* germination reporter was expressed. The luminescent tissue was then imprinted on slides and stained with the spore stain, and frozen sections were prepared for subsequent immunohistochemical analyses. The arrows in panels C and D indicate a nonluminescent caudal mediastinal lymph node. Note that the scales for panels B to D are higher than for panel A and that the photons per second per square centimeter per steradian (luminescence values) are expressed in units $\times 10^3$.

morphologies were not readily distinguishable, although macrophage antigen (CD68) was detectable (Fig. 8D) and colocalized with the vegetative cell antigen signal (Fig. 8E and F). Tissue from uninfected control mice showed no fluorescence with antispore or antivegetative antibodies and no cross-reactivity with labeled secondary antibodies. Furthermore, anti-BclA and anti-EA-1 did not cross-react with vegetative cells or spores, respectively, from in vitro cultures (data not shown). PMNs were also detected in tissue imprints of infected lungs; however, the PMNs appeared somewhat later after challenge with *B. anthracis* spores. Although the PMNs phagocytosed spores, vegetative antigens were only seen in association with macrophages.

Colony counts from infected lung tissue. Aliquots of lung tissue homogenates were cultured directly or following heat treatment to enumerate vegetative cells and spores, or spores alone, respectively. We found that the volume of homogenate diluent influenced the outcome of colony counts. In samples that were homogenized in 1 ml of sterile water, vegetative growth was detected in lung tissue from all nine of the mice tested. The percentage of germination varied from 65 to 94%. When lungs were homogenized in 10 ml of sterile water, we observed significant germination (more than 15%) in five out of eight mice, with the percentage of germination varying from 54 to 81%. The variability seen with different tissue handling techniques suggests that other experimental conditions influence the colony count comparisons, as noted by others (8, 19).

TABLE 2. Phagocytic cell populations from imprints of luminescent lung tissue collected at various times following intranasal infection with *B. anthracis* germination *lux* reporter strain spores[a]

Time postinfection (h)	No. of PMNs	No. of macrophages	No. of PMNs with intracellular spores	No. of macrophages with intracellular spores
0.5	15	26	5	40
1	16	25	1	73
6	556	13	377	13
24	640	24	491	38
48	428	31	377	60

[a] From each tissue sample, two blots were prepared and stained with the Wirtz-Conklin spore stain. Cell counts were obtained by scanning 50 oil immersion fields on each blot. The numbers shown represent the sum of cells of each category seen on the two blots (100 oil immersion fields).

DISCUSSION

Here we describe the construction of a bioluminescent reporter plasmid in which expression of the *lux* operon, driven by the *sspB* promoter, was used to signal the early stages of spore germination in *Bacillus anthracis* Sterne strain. In vitro, *B. anthracis* transformed with the germination reporter showed an initial burst of light emission in broth culture that corresponded with germination. Light emission preceded the expression of the vegetative gene PA and was extinguished during vegetative replication. Mice infected intranasally with Sterne spores derived from the germination reporter strain were monitored with the Xenogen IVIS for light emission, a signal of germination in vivo. The IVIS technology was chosen because the approach is not invasive and the study of ongoing infection is not limited to postmortem analysis. We observed bioluminescence localized to the upper thorax of infected mice; this germination signal was apparent in anesthetized but otherwise-uncompromised mice within 18 h. Dissection of mice at earlier time points showed discrete areas of luminescence in situ in the lungs. These foci of luminescence were seen as early as 6 hours postexposure and prior to further dissection or disturbance of the respiratory tree. The earliest observation of the luminescent germination signal was 30 min postexposure in excised lung tissue. Staining of tissue imprints and frozen sections of bioluminescent lung tissue revealed the presence of extracellular spores and spores within alveolar macrophages. Fluorescent antibody staining confirmed the presence of spores in alveolar macrophages and provided evidence of vegetative growth in infected macrophages. Therefore, under the conditions we used, germination did not appear to occur randomly in the alveolar space, but rather where spores were associated with macrophages. Over time there was a reduction of free spores in the alveolar space. At later time points, numerous PMNs with and without intracellular spores were

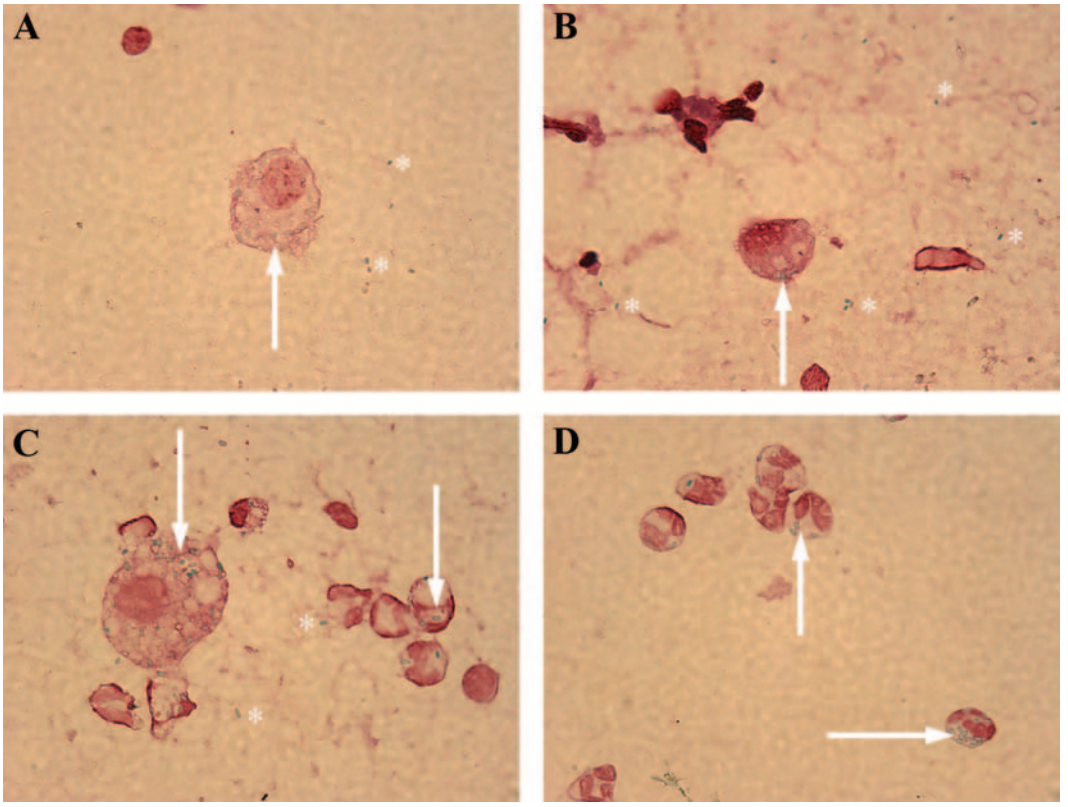

FIG. 6. Wirtz-Conklin spore stains of tissue imprints were prepared from luminescent tissues harvested at 1 h (A and B) and 24 h (C and D) post-intranasal infection with *B. anthracis* transformed with pPS12. (A and B) Tissue imprints taken 1 h postinfection showed macrophages with intracellular malachite green-stained spores (arrows) and extracellular spores (asterisks). (C and D) Tissue imprints made at 24 h postinfection showed macrophages and numerous polymorphonuclear leukocytes with intracellular spores (arrows). Magnification, ×100.

seen, a finding consistent with lung infection involving an inflammatory response. Conventional colony counts of lung tissue homogenate following heat treatment to inactivate vegetative cells provided additional evidence for germination in the lung, but variability in results based on sample processing techniques led us to draw conclusions regarding the site of germination on the bioluminescence and microscopic findings. Our results support observations by Cleret et al. (6) that alveolar macrophages phagocytose most spores in the first 10 minutes of infection, observations by Lyons et al. (25) that germination occurs in the lungs within 1 hour after inoculation, and those by Guidi-Rontani et al. (17), who observed germination in macrophages 30 min after infection.

The controversy over the site and conditions necessary for germination is fueled by many variables in host models, anthrax strains, inoculation routes, and spore handling protocols. Heninger et al. showed that germination, as monitored by colony counts, may be increased when mice are euthanized with CO_2 (19). Other confounding factors could include shifts in the tissue milieu caused by dissection or different anesthesia methods that could alone trigger germination. To minimize these potential sources of error, we used a real-time, quantitative bioluminescence method, genetically timed to generate a signal only during germination in a strain of *Bacillus anthracis* known to be capsule deficient but virulent to A/J mice. Visualization of germination-associated luminescence in whole live mice following inspiration of spores allowed us to determine when germination took place and to localize germination to the lungs. Furthermore, we concluded that the anesthesia we elected to use during spore challenge (isoflurane) did not appear to artificially induce germination, because similar results were observed in a subset of mice sedated with ketamine injected intraperitoneally.

Glomski et al. (14) recently described an encapsulated bioluminescent *B. anthracis* vegetative growth reporter strain in which the *pag* operon was replaced with a promoterless *lux* operon such that the resulting encapsulated strain was nontoxigenic and expressed light under control of the PA promoter. In mice challenged subcutaneously with this vegetative reporter strain, bacterial replication was seen at the site of infection with later involvement of draining lymph nodes and dissemination, even to the lungs. These authors concluded that the temporal distribution of vegetative *lux* expression following subcutaneous inoculation was consistent with germination in the primary site of infection prior to dissemination without a requirement for lymph node involvement. Our observation of germination signal within 20 min of subcutaneous inoculation and only at the site of infection reinforces their conclusions. Together, these studies concur with findings of Bischof et al. (2), who showed that germination occurs 1 to 3 hours after infection and can happen extracellularly at an abraded skin surface before the development of a phagocytic response.

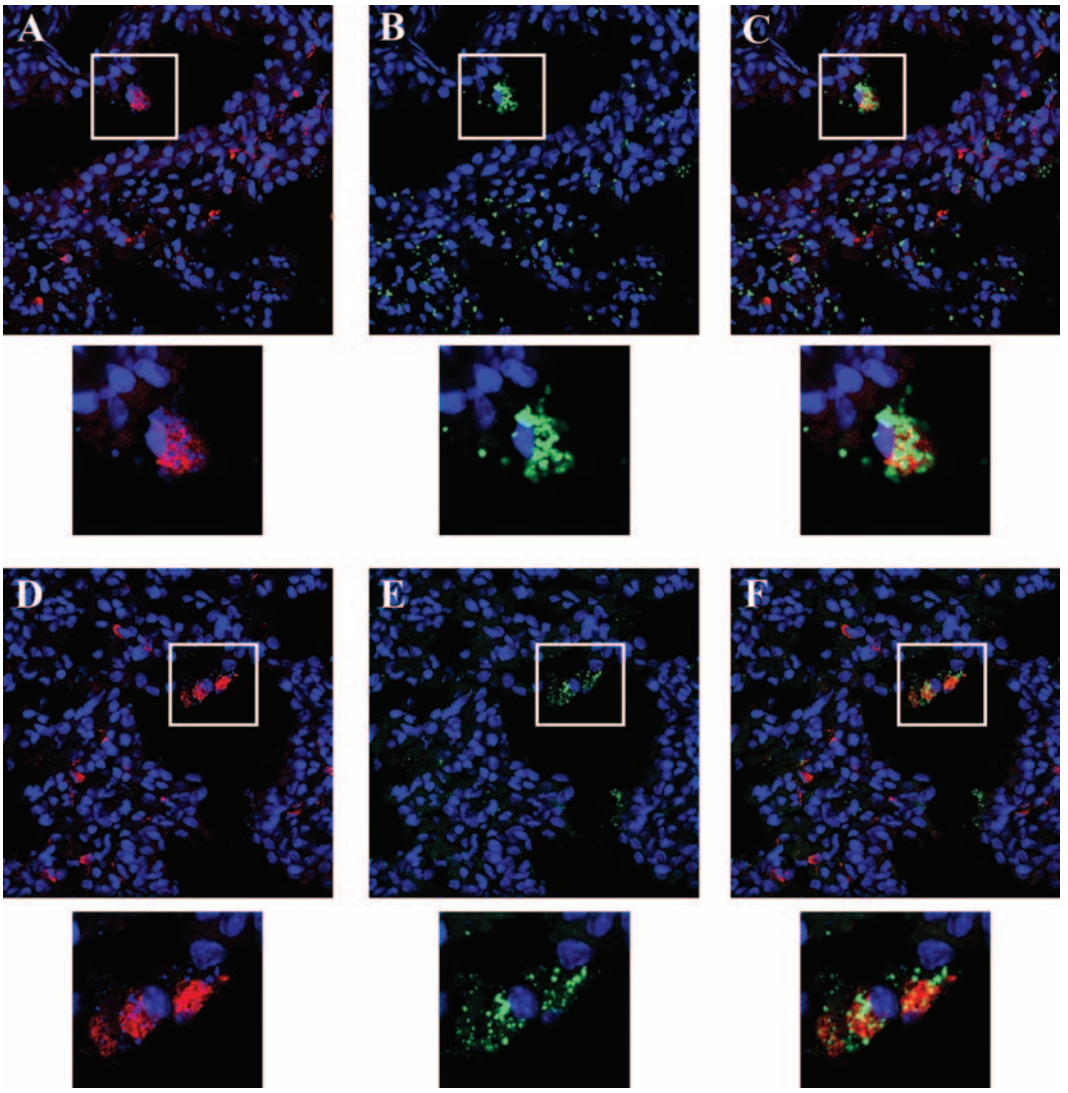

FIG. 7. Immunohistochemistry of frozen sections of luminescent mouse lung tissue harvested 30 min after intranasal inoculation with spores of *B. anthracis* transformed with pPS12. (A to C) Tissue section 1. DAPI nuclear staining (blue) and anti-CD68 macrophage staining (red) show the presence of macrophages in the alveolar space and macrophages within the interstitial tissues (A); DAPI nuclear staining (blue) and anti-BclA spore staining (green) reveal spores in the alveolar space and in the tissues (B); merged images from panels A and B demonstrate spores in association with alveolar macrophages (C). (D to F) Tissue section 2. DAPI nuclear staining (blue) and anti-CD68 macrophage staining (red) again depict the presence of macrophages (D); DAPI nuclear staining (blue) and anti-EA-1 staining (green) illustrate that some vegetative antigen is in the lung at this early time point (E); the merged images from panels D and E show vegetative cell antigen colocalized with macrophages (F). Magnification (A to F), ×63. Inserts below each panel represent enlargement of the boxed area or cell in that panel.

In contrast to our observations, Glomski et al. did not see luminescence in mouse lung tissue following spore challenge by intranasal inoculation. Instead, they observed that replication was confined to the upper respiratory tract, initially in the nasal cavity and later in the mandibular lymph nodes. They also found that intravenously inoculated encapsulated vegetative bacteria reached the lungs rapidly by the hematogenous route and readily multiplied there. These findings were interpreted to support the model of Ross that germination must occur outside the lung and pulmonary colonization follows that extrapulmonary first step. However, the PA-driven reporter strain used by Glomski et al. is luminescent only during vegetative growth, and so the site of germination could not be pinpointed in that work.

We believe that our evidence for germination in the lungs and the disparity between our results and those of Glomski et al. regarding growth in the lungs following intranasal exposure reflect differences between the inhalational models used, the numbers of spores that reached the alveoli, and the differences between the *B. anthracis* strains tested. It was our experience that deeply anesthetized mice, held upright for a few seconds following the inoculation of spores on the nares, inhaled the droplet of spores without swallowing. Hence, very high numbers of spores reached the alveolar spaces. In alert mice inoc-

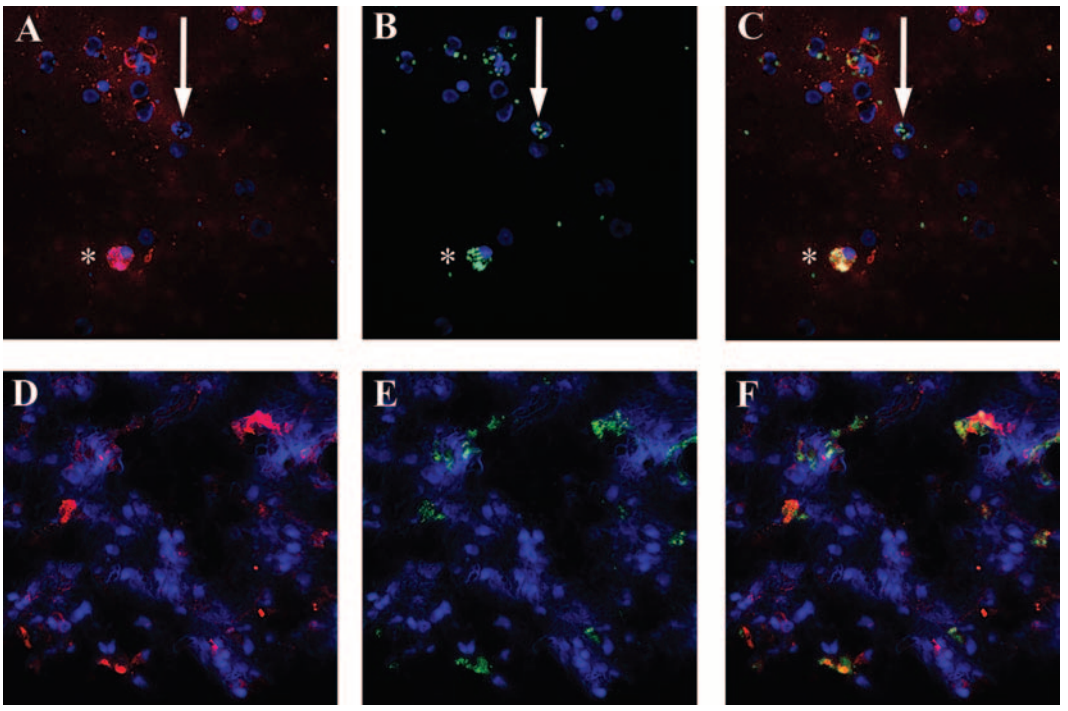

FIG. 8. Immunohistochemistry on tissue imprints or frozen sections of infected luminescent lung tissue taken 48 h postexposure of a mouse to *B. anthracis* spores transformed with pPS12. (A to C) Tissue imprint. DAPI nuclear staining (blue) and anti-CD68 staining (red) indicate that both PMNs (arrow) and macrophages (*) are present (A); DAPI nuclear staining (blue) and anti-BclA spore staining (green) reveal spores associated with nuclear shapes consistent with both macrophages (*) and PMNs (arrow) (B); the merged images from panels A and B demonstrate that spores are present in both macrophages (*) and an unstained cell with a segmented nucleus (arrow) that appears to be a PMN. (D to F) Frozen section. DAPI nuclear staining (blue) and anti-CD68 staining show numerous macrophages in lung tissue (D); DAPI nuclear staining (blue) and anti-EA-1 vegetative cell staining (green) reveal abundant vegetative *Bacillus* antigen (E); the merged images from panels D and E illustrate that vegetative cell antigen colocalizes with macrophages (F). Magnification (panels A to F), ×63. Similar results were obtained with lung samples from four other infected animals.

ulated by nebulization, more spores may become trapped in the upper respiratory tract, which would lead to local germination in the nasal cavity and associated lymphoid tissues with loss of a portion by swallowing. Indeed, in testing our protocol for isoflurane anesthesia, we determined that mice that awoke during the procedure were less likely to demonstrate pulmonary infection. In an inadequately sedated mouse that moved during spore inoculation, bioluminescence was first observed in the region of the lungs; however, luminescence was also seen in the region of the neck, possibly the cervical lymph nodes, and the lower abdomen. We postulated that some spores were swallowed and the resultant luminescence pattern was suggestive of the clinical symptoms of gastrointestinal anthrax, which include sore throat, enlargement of cervical lymph nodes, and soft tissue edema (35). Of course, humans are likely to be alert and upright when exposed inhalationally to spores, and hence the nebulizer model is probably more relevant to human infection. Nonetheless, it is clear from our observations that if numerous spores reach the alveoli, germination ensues at that site in association with macrophages.

The importance of the capsule in dissemination of anthrax is no doubt a factor in the differing observations made in the Glomski study and the results presented here.

Glomski et al. constructed a luminescence reporter strain that is encapsulated but toxin negative. The Sterne strain used in our work is unencapsulated but retains the capacity to produce toxin. Therefore, we observed bioluminescence associated with germination and vegetative growth only in the lungs with our Sterne reporter strains. On the other hand, the encapsulated strain may have disseminated rapidly after germination in the lung, such that the vegetative growth signal in that area was not detectable but was rapidly evident at more distal sites. This theory may also explain the well-accepted findings of Ross, who did not observe germination in the lungs following inhalational challenge and who postulated that spores had to reach the mediastinal lymph nodes after being phagocytosed by alveolar macrophages to germinate and disseminate to other organs. Instead, germination may be followed so rapidly by dissemination that it is only readily visualized in the lung with a capsule-defective reporter strain, such as the Sterne *sspB* reporter we describe here.

We observed that a potential limitation for use of this *sspBp*::*lux* reporter was the reduced germination efficiency of the reporter versus the parent strain. In fact, the higher LD_{50} of the reporter strain was proportional to decreased germination rates seen in the reporter strain (10- to 20-fold). Transformation with the vector backbone led to a partial reduction in the germination efficiency of the reporter strain that we attributed to the metabolic burden inherent in replication of additional episomal DNA. The presence of the *lux* reporter cassette affected germination more significantly. In *Bacillus subtilis*, deletion of *sspB* does not influence the extent of ger-

mination (26); therefore, we speculated that expression of the large *lux* operon and not promoter competition for SspB expression taxed the *Bacillus* host strain. Potential liabilities of Lux expression may include competition for oxygen required for both germination and Lux expression or an additional burden on protein synthesis at a critical step in conversion to the vegetative state.

Another potential drawback to this system is that detection of the germination signal in live infected mice is not very sensitive. Sensitivity was improved and detection hastened by viewing the opened thorax of euthanized infected mice or by excising tissue. Unfortunately, in doing so, the conservation of mice, which is an asset of the IVIS, was circumvented. Nonetheless, the advantage of localization of the luminescent signal within infected tissue without destruction of the tissue architecture is a clear advantage. Furthermore, because the *sspB* promoter-driven *lux* reporter strain provided a luminescent signal exclusively during the early steps in germination, it would be very useful in heavily infected mice for assessment of therapies and vaccines that interfere with germination.

Our studies reinforce the importance of macrophages in the establishment of pulmonary anthrax and prompt additional questions about the spore-macrophage interaction, the role of PMNs and dendritic cells in the host response to *B. anthracis* spores, and how these cells contribute to dissemination of disease. Overall, we share the view expressed by Glomski et al. that passage to regional lymph nodes is not required for germination or establishment of all forms of anthrax. Rather, when *B. anthracis* encounters a hospitable environment, germination and fulminant infection can ensue.

ACKNOWLEDGMENTS

We thank Stephen Davies for sharing his veterinary expertise, Cara Olsen for expert statistical analysis, Thomas Baginski for technical support with confocal microscopy, Micheal Flora for the primer synthesis and DNA sequencing, and Robert Cybulski for assistance with germination assays and for helpful discussions.

This work was supported by NIH/NIAID Middle Atlantic Regional Center of Excellence grant U54 AI057168 and research funds from the United States Navy through the Uniformed Services University grant G173HS.

The opinions and assertions in this paper are the private views of the authors and are not to be construed as official or as reflecting the views of the Department of the Navy or the Department of Defense. This research was conducted in compliance with the Animal Welfare Act. All animal use protocols were reviewed and approved by the Institutional Animal Care and Use Committee of the Uniformed Services University.

REFERENCES

1. **Barlass, P. J., C. W. Houston, M. O. Clements, and A. Moir.** 2002. Germination of *Bacillus cereus* spores in response to L-alanine and to inosine: the roles of *gerL* and *gerQ* operons. Microbiology **148:**2089–2095.
2. **Bischof, T. S., B. L. Hahn, and P. G. Sohnle.** 2007. Characteristics of spore germination in a mouse model of cutaneous anthrax. J. Infect. Dis. **195:**888–894.
3. **Brahmbhatt, T. N., B. K. Janes, E. S. Stibitz, S. C. Darnell, P. Sanz, S. B. Rasmussen, and A. D. O'Brien.** 2007. *Bacillus anthracis* exosporium protein BclA affects spore germination, interaction with extracellular matrix proteins, and hydrophobicity. Infect. Immun. **75:**5233–5239.
4. **Brittingham, K. C., G. Ruthel, R. G. Panchal, C. L. Fuller, W. J. Ribot, T. A. Hoover, H. A. Young, A. O. Anderson, and S. Bavari.** 2005. Dendritic cells endocytose *Bacillus anthracis* spores: implications for anthrax pathogenesis. J. Immunol. **174:**5545–5552.
5. **Cleret, A., A. Quesnel-Hellmann, J. Mathieu, D. Vidal, and J. N. Tournier.** 2006. Resident $CD11c^+$ lung cells are impaired by anthrax toxins after spore infection. J. Infect. Dis. **194:**86–94.
6. **Cleret, A., A. Quesnel-Hellmann, A. Vallon-Eberhard, B. Verrier, S. Jung, D. Vidal, J. Mathieu, and J. N. Tournier.** 2007. Lung dendritic cells rapidly mediate anthrax spore entry through the pulmonary route. J. Immunol. **178:**7994–8001.
7. **Cote, C. K., K. M. Rea, S. L. Norris, R. N. Van, and S. L. Welkos.** 2004. The use of a model of in vivo macrophage depletion to study the role of macrophages during infection with *Bacillus anthracis* spores. Microb. Pathog. **37:**169–175.
8. **Cote, C. K., R. N. Van, and S. L. Welkos.** 2006. Roles of macrophages and neutrophils in the early host response to *Bacillus anthracis* spores in a mouse model of infection. Infect. Immun. **74:**469–480.
9. **Dixon, T. C., A. A. Fadl, T. M. Koehler, J. A. Swanson, and P. C. Hanna.** 2000. Early *Bacillus anthracis*-macrophage interactions: intracellular survival survival and escape. Cell. Microbiol. **2:**453–463.
10. **Drysdale, M., S. Heninger, J. Hutt, Y. Chen, C. R. Lyons, and T. M. Koehler.** 2005. Capsule synthesis by *Bacillus anthracis* is required for dissemination in murine inhalation anthrax. EMBO J. **24:**221–227.
11. **Ezzell, J. W., Jr., and T. G. Abshire.** 1988. Immunological analysis of cell-associated antigens of *Bacillus anthracis*. Infect. Immun. **56:**349–356.
12. **Francis, K. P., D. Joh, C. Bellinger-Kawahara, M. J. Hawkinson, T. F. Purchio, and P. R. Contag.** 2000. Monitoring bioluminescent *Staphylococcus aureus* infections in living mice using a novel *luxABCDE* construct. Infect. Immun. **68:**3594–3600.
13. **Francis, K. P., J. Yu, C. Bellinger-Kawahara, D. Joh, M. J. Hawkinson, G. Xiao, T. F. Purchio, M. G. Caparon, M. Lipsitch, and P. R. Contag.** 2001. Visualizing pneumococcal infections in the lungs of live mice using bioluminescent *Streptococcus pneumoniae* transformed with a novel gram-positive *lux* transposon. Infect. Immun. **69:**3350–3358.
14. **Glomski, I. J., A. Piris-Gimenez, M. Huerre, M. Mock, and P. L. Goossens.** 2007. Primary involvement of pharynx and Peyer's patch in inhalational and intestinal anthrax. PLoS Pathog. **3:**e76.
15. **Guidi-Rontani, C.** 2002. The alveolar macrophage: the Trojan horse of *Bacillus anthracis*. Trends Microbiol. **10:**405–409.
16. **Guidi-Rontani, C., M. Levy, H. Ohayon, and M. Mock.** 2001. Fate of germinated *Bacillus anthracis* spores in primary murine macrophages. Mol. Microbiol. **42:**931–938.
17. **Guidi-Rontani, C., M. Weber-Levy, E. Labruyere, and M. Mock.** 1999. Germination of *Bacillus anthracis* spores within alveolar macrophages. Mol. Microbiol. **31:**9–17.
18. **Hendrickson, D. A., and M. M. Krenz.** 1991. Reagents and stains, p. 1311. *In* A. Balows, W. J. Hausler, Jr., K. L. Herrmann, H. D. Isenberg, and H. J. Shadomy (ed.), Manual of clinical microbiology, 5th ed. ASM Press, Washington, DC.
19. **Heninger, S., M. Drysdale, J. Lovchik, J. Hutt, M. F. Lipscomb, T. M. Koehler, and C. R. Lyons.** 2006. Toxin-deficient mutants of *Bacillus anthracis* are lethal in a murine model for pulmonary anthrax. Infect. Immun. **74:**6067–6074.
20. **Jernigan, D. B., P. L. Raghunathan, B. P. Bell, R. Brechner, E. A. Bresnitz, J. C. Butler, M. Cetron, M. Cohen, T. Doyle, M. Fischer, C. Greene, K. S. Griffith, J. Guarner, J. L. Hadler, J. A. Hayslett, R. Meyer, L. R. Petersen, M. Phillips, R. Pinner, T. Popovic, C. P. Quinn, J. Reefhuis, D. Reissman, N. Rosenstein, A. Schuchat, W. J. Shieh, L. Siegal, D. L. Swerdlow, F. C. Tenover, M. Traeger, J. W. Ward, I. Weisfuse, S. Wiersma, K. Yeskey, S. Zaki, D. A. Ashford, B. A. Perkins, S. Ostroff, J. Hughes, D. Fleming, J. P. Koplan, and J. L. Gerberding.** 2002. Investigation of bioterrorism-related anthrax, United States, 2001: epidemiologic findings. Emerg. Infect. Dis. **8:**1019–1028.
21. **Kadurugamuwa, J. L., L. Sin, E. Albert, J. Yu, K. Francis, M. DeBoer, M. Rubin, C. Bellinger-Kawahara, J. T. Parr, Jr., and P. R. Contag.** 2003. Direct continuous method for monitoring biofilm infection in a mouse model. Infect. Immun. **71:**882–890.
22. **Kang, T. J., M. J. Fenton, M. A. Weiner, S. Hibbs, S. Basu, L. Baillie, and A. S. Cross.** 2005. Murine macrophages kill the vegetative form of *Bacillus anthracis*. Infect. Immun. **73:**7495–7501.
23. **Koehler, T. M., Z. Dai, and M. Kaufman-Yarbray.** 1994. Regulation of the *Bacillus anthracis* protective antigen gene: CO_2 and a *trans*-acting element activate transcription from one of two promoters. J. Bacteriol. **176:**586–595.
24. **Loving, C. L., M. Kennett, G. M. Lee, V. K. Grippe, and T. J. Merkel.** 2007. Murine aerosol challenge model of anthrax. Infect. Immun. **75:**2689–2698.
25. **Lyons, C. R., J. Lovchik, J. Hutt, M. F. Lipscomb, E. Wang, S. Heninger, L. Berliba, and K. Garrison.** 2004. Murine model of pulmonary anthrax: kinetics of dissemination, histopathology, and mouse strain susceptibility. Infect. Immun. **72:**4801–4809.
26. **Mason, J. M., and P. Setlow.** 1986. Essential role of small, acid-soluble spore proteins in resistance of *Bacillus subtilis* spores to UV light. J. Bacteriol. **167:**174–178.
27. **Mayer-Scholl, A., R. Hurwitz, V. Brinkmann, M. Schmid, P. Jungblut, Y. Weinrauch, and A. Zychlinsky.** 2005. Human neutrophils kill *Bacillus anthracis*. PLoS Pathog. **1:**179–186.
28. **Park, H. S., K. P. Francis, J. Yu, and P. P. Cleary.** 2003. Membranous cells in nasal-associated lymphoid tissue: a portal of entry for the respiratory mucosal pathogen group A streptococcus. J. Immunol. **171:**2532–2537.

29. **Reed, L. J., and H. Muench.** 1938. A simple method of estimating fifty percent endpoints. Am. J. Hyg. **27:**493–497.
30. **Ross, J. M.** 1957. The pathogenesis of anthrax following the administration of spores by the respiratory route. J. Pathol. Bacteriol. **73:**485–494.
31. **Ruthel, G., W. J. Ribot, S. Bavari, and T. A. Hoover.** 2004. Time-lapse confocal imaging of development of *Bacillus anthracis* in macrophages. J. Infect. Dis. **189:**1313–1316.
32. **Setlow, B., E. Melly, and P. Setlow.** 2001. Properties of spores of *Bacillus subtilis* blocked at an intermediate stage in spore germination. J. Bacteriol. **183:**4894–4899.
33. **Singh, Y., V. K. Chaudhary, and S. H. Leppla.** 1989. A deleted variant of *Bacillus anthracis* protective antigen is non-toxic and blocks anthrax toxin action *in vivo*. J. Biol. Chem. **264:**19103–19107.
34. **Siragusa, G. R., K. Nawotka, S. D. Spilman, P. R. Contag, and C. H. Contag.** 1999. Real-time monitoring of *Escherichia coli* O157:H7 adherence to beef carcass surface tissues with a bioluminescent reporter. Appl. Environ. Microbiol. **65:**1738–1745.
35. **Sirisanthana, T., and A. E. Brown.** 2002. Anthrax of the gastrointestinal tract. Emerg. Infect. Dis. **8:**649–651.
36. **Smith, J. W., and M. S. Bartlett.** 1991. Diagnostic parasitology: introduction and methods, p. 712. *In* A. Balows, W. J. Hausler, Jr., K. L. Herrmann, H. D. Isenberg, and H. J. Shadomy (ed.), Manual of clinical microbiology, 5th ed. ASM Press, Washington, DC.
37. **Sylvestre, P., E. Couture-Tosi, and M. Mock.** 2002. A collagen-like surface glycoprotein is a structural component of the *Bacillus anthracis* exosporium. Mol. Microbiol. **45:**169–178.
38. **Van den Broeck, W., A. Derore, and P. Simoens.** 2006. Anatomy and nomenclature of murine lymph nodes: descriptive study and nomenclatory standardization in BALB/cAnNCrl mice. J. Immunol. Methods **312:**12–19.
39. **Welkos, S., A. Friedlander, S. Weeks, S. Little, and I. Mendelson.** 2002. *In-vitro* characterisation of the phagocytosis and fate of anthrax spores in macrophages and the effects of anti-PA antibody. J. Med. Microbiol. **51:**821–831.
40. **Welkos, S. L., C. K. Cote, K. M. Rea, and P. H. Gibbs.** 2004. A microtiter fluorometric assay to detect the germination of *Bacillus anthracis* spores and the germination inhibitory effects of antibodies. J. Microbiol. Methods **56:** 253–265.
41. **Welkos, S. L., T. J. Keener, and P. H. Gibbs.** 1986. Differences in susceptibility of inbred mice to *Bacillus anthracis*. Infect. Immun. **51:**795–800.
42. **Williams, D. D., and C. L. Turnbough, Jr.** 2004. Surface layer protein EA1 is not a component of *Bacillus anthracis* spores but is a persistent contaminant in spore preparations. J. Bacteriol. **186:**566–569.

Editor: R. P. Morrison